fishes

MDPI

Article

Blood Transcriptome Analysis Provides Responsive Changes in Gene Expression between Ex Situ and Captive Yangtze Finless Porpoises (*Neophocaena asiaeorientalis asiaeorientalis*)

Zhichen Cao [1,†], Denghua Yin [2,†], Zhanwei Li [3,†], Yan Yan [4,†], Peng Zhang [3], Sigang Zhang [4], Danqing Lin [2], Zhong Hua [2], Jialu Zhang [2], Congping Ying [5], Han Zhang [1], Pao Xu [2,5], Guixin Dong [6,*] and Kai Liu [1,2,5,*]

1 National Demonstration Center for Experimental Fisheries Science Education, Shanghai Ocean University, Shanghai 201306, China
2 Key Laboratory of Freshwater Fisheries and Germplasm Resources Utilization, Ministry of Agriculture and Rural Affairs, Freshwater Fisheries Research Center, Chinese Academy of Fishery Sciences, Wuxi 214081, China; xup@ffrc.cn (P.X.)
3 Zhuhai Chimelong Investment and Development Co., Ltd., Zhuhai 519000, China
4 Anqing Aquatic Technology Promotion Center Station, Anqing 246000, China; matthew956@163.com (Y.Y.)
5 Wuxi Fisheries College, Nanjing Agricultural University, Wuxi 214081, China
6 Guangdong South China Rare Wild Animal Species Conservation Center, Zhuhai 519031, China
* Correspondence: dgx@chimelong.com (G.D.); liuk@ffrc.cn (K.L.)
† These authors contributed equally to this work.

Abstract: The Yangtze finless porpoise (*Neophocaena asiaeorientalis asiaeorientalis*, YFP) is an endangered species endemic to the Yangtze River in China, and it is the only freshwater whale in the genus Neophocaena. In terms of protection, three effective conservation strategies exist: in situ conservation, ex situ conservation, and artificial breeding, all of which have been implemented by the Chinese government. Of these, ex situ conservation involves the relocation of Yangtze finless porpoises to semi-natural waters with less human interference, and artificial breeding involves the relocation of Yangtze finless porpoises to a controlled environment that is more strictly managed. To compare and analyze the responsive changes in gene expression of the YFPs between the ex situ and controlled environments, we performed the RNA sequencing of blood tissues from these YFPs. A total of 1201 differentially expressed genes (DEGs) were identified, of which 423 were up-regulated in the ex situ population and 778 were up-regulated in the controlled-environment population. Gene enrichment analysis showed that 1201 DEGs between the ex situ and controlled-environment populations were generally enriched for vision-, digestion- and immune-system-related pathways. Further analysis revealed that several key immune system pathways, such as the chemokine signaling pathway and B cell receptor signal pathway, were activated in the ex situ population. In addition, the key pathways related to vision, including phototransduction and the inflammatory mediator regulation of TRP channels, as well as the pathways related to the digestive system, such as protein digestion and absorption and salivary secretion, were activated in the controlled-environment population. These results suggest that the ex situ populations may respond to complex environmental conditions in semi-natural waters by enhancing their immune function through the increased expression of immune-related genes and that the visual function and protein digestion of the YFPs were improved compared to those of the ex situ population based on the conditions of artificial feeding, such as the higher transparency of the water and regular feeding. This study provides clues for evaluating the adaptability of YFPs to different environments and is a useful reference for future ex situ conservation and artificial breeding.

Keywords: Yangtze finless porpoise; environment; blood; visual; digestive system; immune system

Key Contribution: In this study, we conducted transcriptomics analysis on the blood tissues of four YFPs transferred from ex situ waters to a controlled environment, and we explored the responsive changes in gene expression in the YFPs under different environmental conditions, with a view to provide technical support for the ex situ conservation of YFPs and artificial breeding.

Citation: Cao, Z.; Yin, D.; Li, Z.; Yan, Y.; Zhang, P.; Zhang, S.; Lin, D.; Hua, Z.; Zhang, J.; Ying, C.; et al. Blood Transcriptome Analysis Provides Responsive Changes in Gene Expression between Ex Situ and Captive Yangtze Finless Porpoises (*Neophocaena asiaeorientalis asiaeorientalis*). *Fishes* **2023**, *8*, 593. https://doi.org/10.3390/fishes8120593

Academic Editor: Giacomo Zaccone

Received: 15 October 2023
Revised: 23 November 2023
Accepted: 24 November 2023
Published: 30 November 2023

1. Introduction

The Yangtze finless porpoise (*Neophocaena asiaorientalis asiaorientalis*, YFP) is a small-toothed whale endemic to China, found only in the middle and lower reaches of the Yangtze River as well as in the adjacent Dongting and Poyang Lakes. It serves as a crucial indicator species for assessing the health of the freshwater Yangtze River ecosystem and the state of its biodiversity [1]. Unfortunately, the YFP population faces numerous threats, including the threat of intensive shipping, sand mining, dams and other water-related engineering construction projects, and the pollution of the Yangtze River water environment. As a result, the YFP population has declined significantly, from around 2700 in the early 1990s to approximately 1249 in 2022 [2]. Given the endangered status of the YFP population, the International Union for the Conservation of Nature's Species Survival Commission (IUCN/SSC) classified YFPs as "Critically Endangered" (CR) in 2013 [3]. On 5 February 2021, the adjusted "List of National Key Protected Wild Animals" listed YFPs as a national first-class protected wild animal, further increasing the demand their protection. Although the rapid decline in the population of YFPs has been curbed, the situation has not changed, and protection remains essential. Therefore, the protection of and research about YFPs are urgently needed.

Since the 1980s, China has gradually explored three major conservation strategies for YFPs: in situ conservation, ex situ conservation, and artificial breeding [4]. Establishing a suitable ex situ conservation population in selected waters has proven to be a direct and effective method of protecting YFPs [5]. Furthermore, relocating YFPs to aquariums with state-of-the-art facilities and expertise in caring for, raising, and breeding cetaceans in captivity is the most effective means of avoiding their extinction. Currently, China houses five ex situ conservation and two controlled-environment populations [6]. In ex situ waters, there is less human activity and abundant fish resources, but the water quality conditions are affected by the neighboring residents' activities and farmland drainage [7]. For instance, in the semi-natural protected waters of Tongling, Mi detected triple nitrogen and E. coli, exceeding the required range for captive pools [8]. In contrast, the captive bases have more comprehensive facilities, and the water in the captive pools is continuously treated using a livelihood system. A professional water quality testing team monitors the water daily, ensuring that all the water quality indicators meet the required standards for the animals' survival [9].

Previous research has shown that different environments can have significant effects on the metabolism [10], immunity [11], and sensory systems [12] of YFPs. Lin Gang et al. found that the rate of amino acid metabolism in a controlled-environment population was significantly higher than that in a wild population [10], which might be mainly due to the fact that the wild YFPs had a high activity level, and a large amount of amino acids in the blood were used by the muscle tissues. Nabi et al. (2019) found that the controlled environment affected the immune system of the YFPs, and that compared with the group from the old channel of the Tian'ezhou National Natural Reserve, the relative expression of immune genes in the group from Poyang Lake was lower [10]. Additionally, Liu (2022) analyzed the blood transcriptome of YFPs and found that there were significant differences in auditory functions between the relocated and natural populations [12]. However, there are still fewer studies on the effects of the environment on YFPs, and even fewer studies involving the transcriptomics of YFPs. In addition, fresh tissues of rare and protected species such as the YFP are extremely difficult to obtain, and scholars often use blood tissues collected without causing damage instead of the other tissues for transcriptome studies. Shen et al. (2019) explored the cause of baldness in pandas through studying the blood transcriptome and found that the hair-promoting factor Wnt10b was significantly down-regulated and expressed in the blood of pandas with baldness [13]. Liu (2017) performed the comparative analysis of the blood transcriptome of high-altitude and low-altitude wolves and found that the differentially expressed genes in the blood of the two

wolves were significantly enriched in the hypoxia response, aerobic respiration, and ATP metabolism pathways, so as to adapt to the environment at different altitudes [14]. In this study, we conducted mRNA sequencing and analysis of the blood tissues of four YFPs from semi-natural ex situ waters that were moved to a controlled environment. By constructing an expression profile of the mRNAs in blood tissues and conducting differential gene expression and enrichment analyses, we identified the key DEGs and pathways. This study aimed to explore the responsive changes in the gene expression levels of YFPs living in the two different environments, providing a theoretical basis and reference materials for the future ex situ protection and artificial breeding of YFPs.

2. Materials and Methods

2.1. Ethics Statement

We strictly followed the national regulations and policies for animal protection in China. The medical examinations and related experiments conducted were approved by competent authorities of the Department of Resource Environmental Protection, Yangtze River Basin Fisheries Regulation and Management Office, Ministry of Agriculture. Which reviewed and approved the procedures for animal chasing, handling, and blood collection (2017 [185] and 2018 [183]).

2.2. Animals and Samples Collection

In May 2018, we collected blood from four YFPs with an average age of 6 years old (EW1♂, EW2♀, EW4♀, and EW4♂) for experimental analysis while implementing a health checkup in the Anqing Xijiang Yangtze Finless Porpoise Ex Situ Protected Waters (EW, ex situ waters). In August of the same year, with the approval of the competent authorities, the same four YFPs (CL1♀, CL2♂, CL3♂, and CL4♀) were relocated to the Zhuhai Chimelong Yangtze Finless Porpoise Artificial Breeding and Science Popularization Education Base (CL, controlled environment). In October 2020, we collected blood samples from these four YFPs during a health checkup in the Chimelong Artificial Breeding Waters for analysis. See Table S1 for more information on laboratory animals. The Anqing Xijiang Yangtze Finless Porpoise Ex situ Protected Waters has a total length of about 9 km, a water surface width of about 300 m, an average water depth of about 8.7 m, and a maximum water depth of more than 20 m. Both sides of the river are natural shorelines, and the ecological environment and management conditions of the waters are excellent. The Zhuhai Chimelong Yangtze Finless Porpoise Artificial Breeding and Science Popularization Education Base is located in Zhuhai Chimelong Ocean Kingdom. The YFPs breeding pool is filled with tap water sterilized with ozone and chlorine and is equipped with water pumps for its filtration and circulation.

We used the traditional "sound chase and net capture" method [15] (Hao et al., 2009) to capture the animals in batches. The follow-up physical examination and blood collection can only be carried out when the animals gently come out of the water, move freely, and are not obviously stressed. During blood collection, we used a 10 mL disposable syringe to extract blood from the main vein of the Yangtze finless porpoise tails, and then transferred the blood samples into PAXgene Blood RNA Tubes (BD, Franklin Lakes, NJ, USA), which were transported back to the laboratory and stored in an ultra-low-temperature refrigerator at −80 °C for use.

2.3. Experimental Methods

2.3.1. Library Construction and Sequencing

Total RNA was extracted from 8 blood samples using the PAXgene Blood RNA kit (QIAGEN, Hilden, Germany). We used Agilent 2100 Bioanalyzer (Agilent, Santa Clara, CA, USA) to perform quality inspection of the extracted Total RNA. After passing the quality inspection, we enriched the mRNA with polyA tail using magnetic beads with OligodT. And then, we added an appropriate amount of interruption reagent to the obtained mRNA to fragment it under high-temperature conditions. We used interrupted mRNA as a

template to synthesize the first-strand cDNA, and then configured the two-strand synthesis reaction system to synthesize the second-strand cDNA. And we used the kit to purify the recovered end repair, added base "A" to the 3′ end of the cDNA, connected the linker, and then selected the size of the fragment. And finally, we performed PCR amplification. The quality of the constructed library was checked, and sequencing was performed after passing. High-throughput sequencing was conducted using the BGISEQ-500 platform (BGI, Shenzhen, China) with 150 bp paired-end reads.

2.3.2. Sequencing Data Filtering Analysis

We used SOAPnuke (v1.4.0, BGI Gene) software for filtering to obtain valid data (clean data). The specific steps are as follows:

(1) Remove the reads with a sequencing adapter;
(2) Remove the reads with an unknown base N content greater than 5%;
(3) Remove the low-quality reads (reads with bases with a mass value below 15, accounting for more than 20% of the total base number of the reads).

Subsequently, the filtered clean reads were annotated and analyzed with the YFP reference genome (*Neophocaena_asiaeorientalis*_V1.1., https://www.ncbi.nlm.nih.gov/genome/?term=Neophocaena%2520asiaeorientalis, accessed on 15 November 2021) [1] using HISAT2 (v2.1.0) [16] software.

2.3.3. Differential Expression Analysis and Enrichment Analysis

We used DEGseq [17] for the differential expression analysis of the sequenced genes. We normalized the data and screened the DEGs using $|\log2\ \text{Fold Change}| \geq 1$ and p value ≤ 0.05 as conditions. Based on the GO and KEGG annotation results, we categorized the DEGs into functional and biological pathways.

Enrichment analysis is a widely used bioinformatics analysis method for determining whether a set of genes or proteins is enriched for a particular function or pathway. It infers the extent to which these genes are enriched for specific functions or pathways by comparing the differences between the set of study genes and a background set. We performed enrichment analysis using the phyper function in R software to calculate the p value and considered the pathway, with a p value ≤ 0.05 being significantly enriched. The p value was calculated as follows:

$$p\ value = 1 - \sum_{j=0}^{x-1} \frac{\binom{M}{j}\binom{N-M}{n-j}}{\binom{N}{n}}$$

N represents the number of genes involved in GO/KEGG annotation in all the genes; n represents the number of differentially expressed genes (DEGs) in N; M represents the number of genes annotated in a particular GO term/KEGG pathway in all the genes; and x represents the number of DEGs annotated in a particular GO term/KEGG pathway [18].

2.3.4. Validation of RT-qPCR

In order to verify the accuracy of the obtained DEGs, we randomly selected 9 DEGs for real-time fluorescence quantitative PCR (SYBR green fluorescent dye method). And we selected *GAPDH* (glyceraldehyde 3-phosphate dehydrogenase) as the internal reference gene. Primer sequences were then designed using Primer Premier 5.0 (Permier Biosoft, San Francisco, CA, USA) for qRT-PCR (Table 1). And we produced amplification and melting curves to test the specificity of the primers (Figures S1 and S2). The relative expression of genes was calculated using the $2^{-\Delta\Delta CT}$ method. The specific steps are as follows:

(1) Reverse-transcription of the tested RNA at 500 ng was performed at the following reaction temperatures and reaction times: 25 °C for 10 min; 50 °C for 30 min; 85 °C for 5 min, and left at −20 °C for storage after the end of the reaction;

(2) Dilute the cDNA obtained in step 1 by 5-fold, and configure the qPCR reaction (Table S2);
(3) Set the cycling conditions (Table S3).

Table 1. RT-qPCR primers.

Gene Name	Gene ID	Full Name	Forward Primer (5′-3′)	Reverse Primer (5′-3′)
GAPDH	112391848	glyceraldehyde 3-phosphate dehydrogenase	AGGTCGGAGTGAACGGATTT	TTCTCAGCCTTGACTGTGCC
PDLIM1	112409851	PDZ and LIM domain 1	GGCATTGTCGGCGTGTTT	GCCCTTCTGTTTCAGGTTCG
RHO	112407247	rhodopsin	TCGCCAGAGGTCAACAATG	AGCAGATCAGGAAAGCAACG
SLC51B	112393149	SLC51 subunit beta	GAAACTCACAGCCCTTCTTAGC	CAAAGTTACAGGAGTGGCGAA
TRPC1	112415902	transient receptor potential cation channel subfamily C member 1	AAAAGGACAGCCTCCGACAT	CACCTCCACAAGGCTTAGTTCT
CAMK2D	112400110	calcium/calmodulin dependent protein kinase II delta	ACCCTGCCAAGCGTATCAC	TTTCTTCAAGCAGTCAACAGTCTC
NOS1	112408771	nitric oxide synthase 1	CTCGTTTCCTCAAGGTCAAGA	GCTTTGGAGCCGAATCTTT
EFCAB7	112412952	EF-hand calcium binding domain 7	GAAGAAATCCATCCCAAAAGAC	GTGTGTAAAATAGAGCCATCATCAT
PRKACB	112415075	protein kinase cAMP-activated catalytic subunit beta	TCTCAGCAAGGGCTACAATAAG	TCCAAACCGCTTCGTCAG
ISOC1	112407775	isochorismatase domain containing 1	AGGTTCAGACCAGCCATCAA	CCAAATAACACAACACTCCTGACT

3. Results

3.1. Analysis of Sequencing Data

In this study, we sequenced approximately 691 million raw reads from eight blood samples of YFPs (Table 2). And after removing reads with a sequencing adapter, with an 'N' base ratio over 5% and low-quality base ratio over 20%, about 680 million clean reads remained. The average length of the clean reads in the EW group amounted to 76.30 Gb, and the average length of clean reads in the CL group amounted to 93.71 Gb. And the filtered reads had an average base quality value of Q20 (98.67%) and Q30 (94.81%), indicating that the sequencing data in this study had a high base reading accuracy. Comparing the clean reads of eight samples using HISAT2 to the reference genome (MKKW000000), an average of 75,368,757 reads (88.66%) per sample were found. And the average alignment rate of single mapped reads is 83.93% (Table 2), indicating the high reliability of the sequencing data in this study.

Table 2. Summary of mRNA-seq results of blood samples from Yangtze finless porpoises.

Sample	Total Raw Reads (M)	Total Clean Reads (M)	Total Clean Bases (Gb)	Clean Reads Q20 (%)	Clean Reads Q30 (%)	Clean Reads Ratio (%)	Total Mapping (%)	Uniquely Mapping (%)
EW1	63.1	61.74	9.26	98.67	94.89	97.84	84.16	77.52
EW2	58.01	56.54	8.48	98.77	95.27	97.47	81.55	73.02
EW4	103.11	101.93	15.29	98.62	94.66	98.85	92.49	89.18
EW4	87.03	85.01	12.75	98.6	94.59	97.68	87.72	83.1
CL1	96.89	95.72	14.36	98.69	94.91	98.79	92.41	89.09
CL2	103.11	101.9	15.28	98.62	94.67	98.82	92.1	88.81
CL3	85.81	84.7	12.71	98.64	94.73	98.71	89.23	84.98
CL4	93.86	92.53	13.88	98.66	94.79	98.58	89.61	85.72

3.2. Differential Expression Gene Analysis and Functional Annotation

After performing the differential expression analysis of the transcriptome data, a Venn diagram of gene expression showed no significant difference in most of the gene expression amounts between the EW and CL groups (Figure 1A). However, upon applying the criteria of $|\log2 \text{ Fold Change}| \geq 1$ and p value ≤ 0.001, a total of 1201 differentially expressed

genes (DEGs) were identified (Table S4). Among these, 778 DEGs were up-regulated in the CL group, while 423 DEGs were up-regulated in the EW group (Figure 1B). These findings suggest that environment changes may indeed influence the mRNA expression profile of the YFPs.

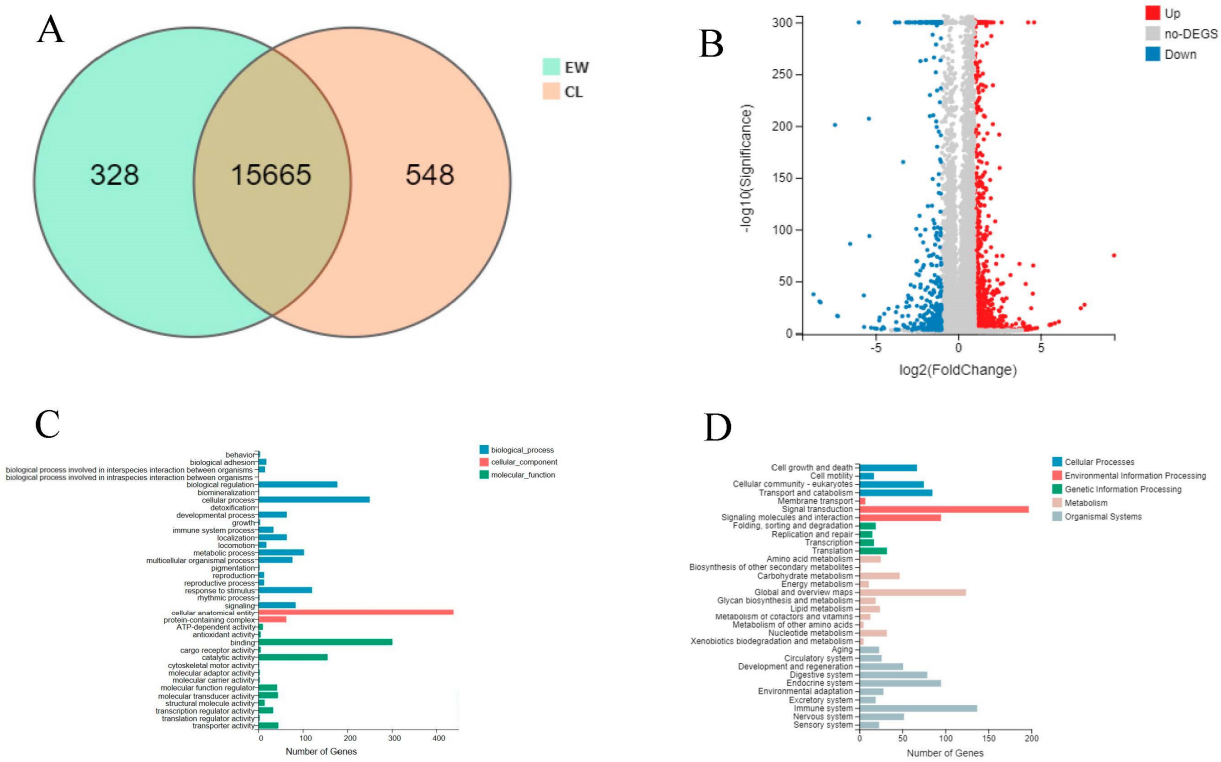

Figure 1. Venn plot of gene expression. (**A**) Scatter plot of differential genes. (**B**) GO classification (**C**) and KEGG classification (**D**) of 1201 DEGs between ex situ and controlled environment populations.

To further understand the functional implications of the DEGs, we conducted GO database analysis for functional annotation and classification. A total of 695 DEGs were annotated, comprising 293 cellular process, 155 immune system process, and 140 responses to stimuli (Figure 1C). Additionally, 588 DEGs were annotated in the KEGG database, with 17 related to the sensory system, 69 related to the digestive system, and 135 related to the immune system (Figure 1D). These results indicate that the YFPs might undergo physiological regulation to respond to different environments.

3.3. Enrichment Analysis of Differentially Expressed Genes

The GO enrichment analysis results demonstrate that the DEGs were significantly enriched in 270 GO entries (Table S5), and Figure 2A shows the 20 GO terms with the most significant enrichment degree. Among them, the immunity-related pathways, such as *defense response to bacteria* and *T cell receptor diversity*, were significantly enriched. The KEGG enrichment analysis results reveal the significant enrichment of 49 pathways (Figure S3), and Figure 2B illustrates the top 20 pathways, which were mainly in pathways related to the vision, digestion, and immune systems (Table 3).

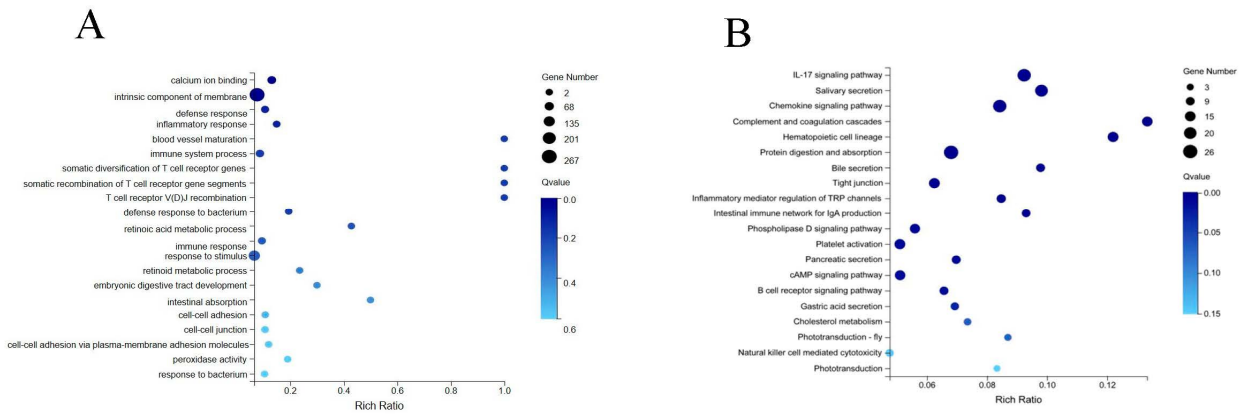

Figure 2. GO enrichment bubble map (**A**) and KEGG pathway enrichment bubble map (**B**) of 1201 DEGs between ex situ and controlled environment populations. *x*-axis: rich ratio, number of DEGs enriched in this pathway/number of all DEGs used for enrichment analysis; *y*-axis: the name of KEGG pathways; bubble color: *p* value, indicating the degree of enrichment significance, the deeper the color is, the smaller the *p* value is, and the higher the degree of enrichment is; bubble size: number of DEGs enriched in the pathway.

Table 3. Enrichment pathways of DEGs related to visual, digestive, and immune systems of YFPs in ex situ and controlled environments.

Pathway ID	Pathway Name	*p* Value
	Visual-system-related pathway	
ko04750	inflammatory mediator regulation of TRP channels	2.32×10^{-4}
ko04745	phototransduction—fly	1.71×10^{-2}
ko04744	phototransduction	4.24×10^{-2}
	Digestive-system-related pathway	
ko04970	salivary secretion	6.23×10^{-9}
ko04974	protein digestion and absorption	1.87×10^{-7}
ko04976	bile secretion	1.61×10^{-4}
ko04972	pancreatic secretion	1.91×10^{-3}
ko04971	gastric acid secretion	6.23×10^{-3}
	Immune-system-related pathways	
ko04657	IL-17 signaling pathway	3.66×10^{-9}
ko04062	chemokine signaling pathway	2.12×10^{-8}
ko04610	complement and coagulation cascades	5.15×10^{-8}
ko04640	hematopoietic cell lineage	5.74×10^{-8}
ko04672	intestinal immune network for IgA production	5.27×10^{-4}
ko04611	platelet activation	1.79×10^{-3}
ko04662	B cell receptor signaling pathway	2.88×10^{-3}

3.4. Analysis of Key Genes and Pathways

The enrichment analysis results reveal the differential expression of the vision-, digestion-, and immune-related genes in the YFPs under different environment conditions. Several vision-related genes, such as *RHO* (rhodopsin) and *EFCAB7* (EF-hand calcium binding domain 7), and activated vision-related pathways, such as phototransduction and the inflammatory mediator regulation of TRP channels, were significantly up-regulated in the CL group. In addition, several key digestive genes, such as *COL4A2* (collagen type IV alpha 2 chain) and *COL5A2* (collagen type V alpha 2 chain), and activated protein digestion and absorption, protein synthesis and absorption, and other digestive system-related pathways were also significantly up-regulated in the CL group. Furthermore, several immune-related genes, like *C1S* (complement C1s) and *CCR10* (C-C motif chemokine receptor 10), were significantly up-regulated in the EW group. The expression was significantly up-regulated

in the complement and coagulation cascade, chemokine signaling pathway, B-cell receptor signaling pathway, and other immune system-related pathways.

Further analysis revealed that most of the vision- and digestion-related pathways were activated in the CL group, while most of the immune system-related pathways were activated in the EW group (Figure 3A).

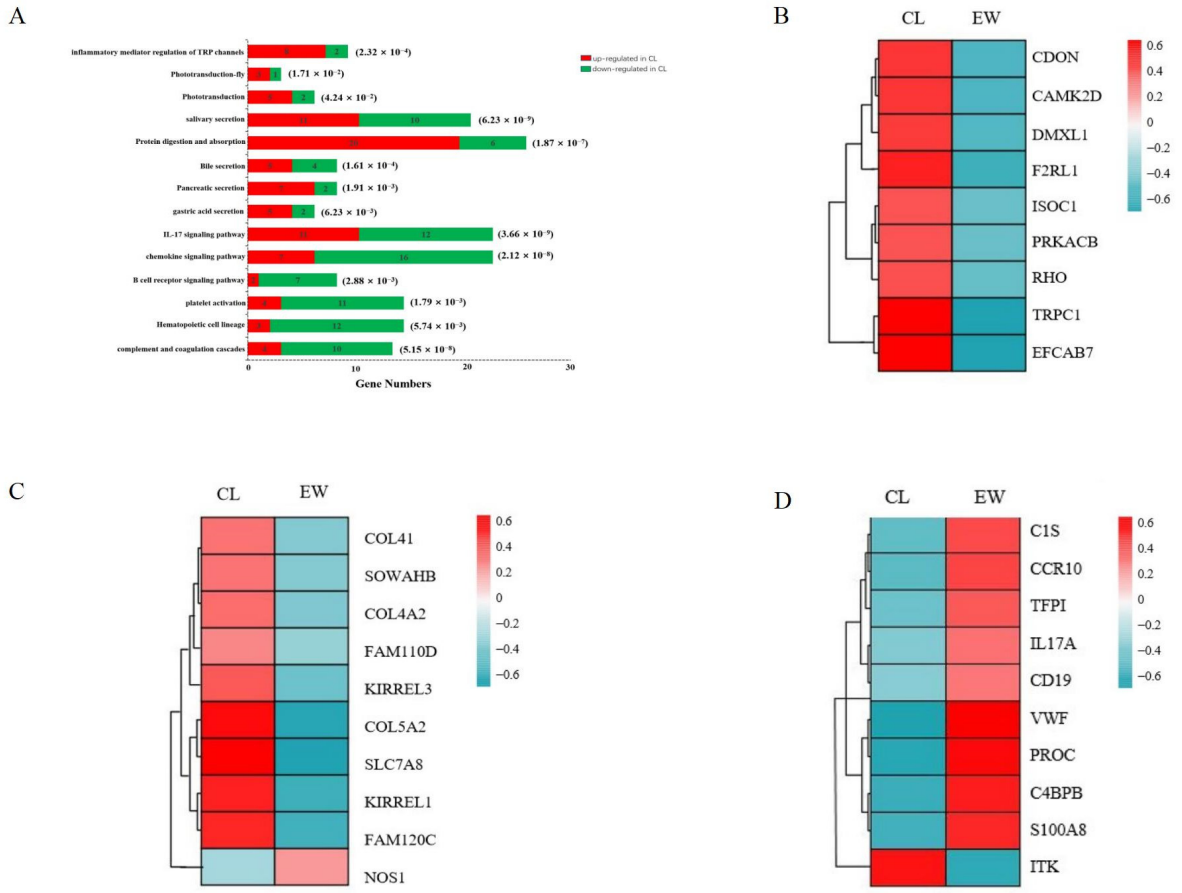

Figure 3. Number of key pathway differential genes (**A**) and heat maps of genes related to vision (**B**), digestive system (**C**), and immune system (**D**). The control group is the EW group, while the experimental group is the CL group. The numbers in parentheses in Figure B represent the *p value*. The changes in the grids from dark red to dark blue in the heat maps indicate the DEG expression from high to low, respectively.

Considering that the enrichment analysis results revealed the differential expression of the vision-, digestion-, and immune-related genes in the YFPs under different environment conditions, we combined many literature reviews [19–25] to screen for these DEGs in the EW and CL groups (Table 4, more information on the genes screened is given in Table S6, KEGG enrichment analysis of the screened genes is shown in Table S7). We performed the cluster analysis of these DGEs and found that among them, the vision- and digestion-related genes were almost all up-regulated and expressed in the CL group (Figure 3B,C), whereas most of the immune system-related genes were up-regulated in the EW group (Figure 3D).

Table 4. DEGs related to vision, digestion, and immune systems.

Category	Gene Name	Gene ID	Full Name	log2 (CL/EW)	*p*-Value
Visual-related genes	*RHO*	112407247	rhodopsin	1.44	5.63×10^{-4}
	EFCAB7	112412952	EF-hand calcium binding domain 7	1.54	9.42×10^{-6}
	DMXL1	112398650	Dmx like 1	1.20	8.32×10^{-39}
	CAMK2D	112400110	calcium/calmodulin dependent protein kinase II delta	1.03	2.52×10^{-33}
	F2RL1	112391430	F2R like trypsin receptor 1	1.83	9.39×10^{-5}
	ISOC1	112407775	isochorismatase domain containing 1	1.10	5.63×10^{-18}
	PRKACB	112415075	protein kinase cAMP-activated catalytic subunit beta	1.00	2.92×10^{-95}
	TRPC1	112415902	transient receptor potential cation channel subfamily C member 1	1.94	6.99×10^{-11}
	CDON	112396881	cell adhesion molecule-related/down-regulated by oncogenes	1.89	8.13×10^{-6}
Digestive-system-related genes	NOS1	112408771	nitric oxide synthase 1	−1.83	2.66×10^{-136}
	COL4A2	112405545	collagen type IV alpha 2 chain	1.00	1.56×10^{-20}
	COL5A2	112392120	collagen type V alpha 2 chain	1.03	2.09×10^{-10}
	COL4A1	112405565	collagen type IV alpha 1 chain	1.35	6.09×10^{-6}
	KIRREL3	112396840	kirre like nephrin family adhesion molecule 3	1.00	2.31×10^{-4}
	KIRREL1	112403475	kirre like nephrin family adhesion molecule 1	1.05	3.26×10^{-3}
	SLC7A8	112397487	solute carrier family 7 member 8	1.23	3.17×10^{-95}
	SOWAHB	112405618	sosondowah ankyrin repeat domain family member B	1.51	5.02×10^{-39}
	FAM110D	112414353	family with sequence similarity 110 member D	1.71	7.49×10^{-5}
	FAM120C	112414621	family with sequence similarity 120C	1.06	2.19×10^{-37}
Immune-system-related genes	*C1S*	112391771	complement C1s	−2.78	3.02×10^{-3}
	CCR10	112399840	C-C motif chemokine receptor 10	−1.85	3.59×10^{-4}
	PROC	112395009	protein C, inactivator of coagulation factors Va and VIIIa	−1.79	9.03×10^{-8}
	IL17A	112414006	interleukin 17A	−1.76	6.98×10^{-12}
	C4BPB	112403521	complement component 4 binding protein beta	−1.36	6.54×10^{-4}
	VWF	112391767	von Willebrand factor	−1.22	4.27×10^{-17}
	TFPI	112400364	tissue factor pathway inhibitor	−1.14	5.13×10^{-4}
	CD19	112399325	CD19 molecule	−1.07	5.67×10^{-66}
	S100A8	112401769	S100 calcium binding protein A8	−1.17	0
	ITK	112409812	IL2 inducible T cell kinase	1.24	0

3.5. Validation of RNA-Seq Results via qRT-PCR

In this study, we randomly selected nine differentially expressed genes for qRT PCR validation. The results showed that, compared to the EW group, the *RHO* (rhodopsin), *TRPC1* (transient receptor potential cation channel subfamily C member 1), *CAMK2D* (calmodulin-dependent protein kinase II delta), *EFCAB7* (EF-hand calcium binding domain 7), *PRKACB* (protein kinase cAMP-activated catalytic subunit beta) and *ISOC1* (isochorismatase domain containing 1) genes were up-regulated in the CL group, while *PDLIM1* (PDZ and LIM domain 1), *SLC51B* (SLC51 subunit beta), and *NOS1* (nitric oxide synthase 1) genes were down-regulated in the CL group (Figure 4). The comparison of the qRT PCR validation and transcriptome sequencing results revealed that the trends in the gene expression levels were essentially the same, indicating that the transcriptome sequencing results in this study are reliable.

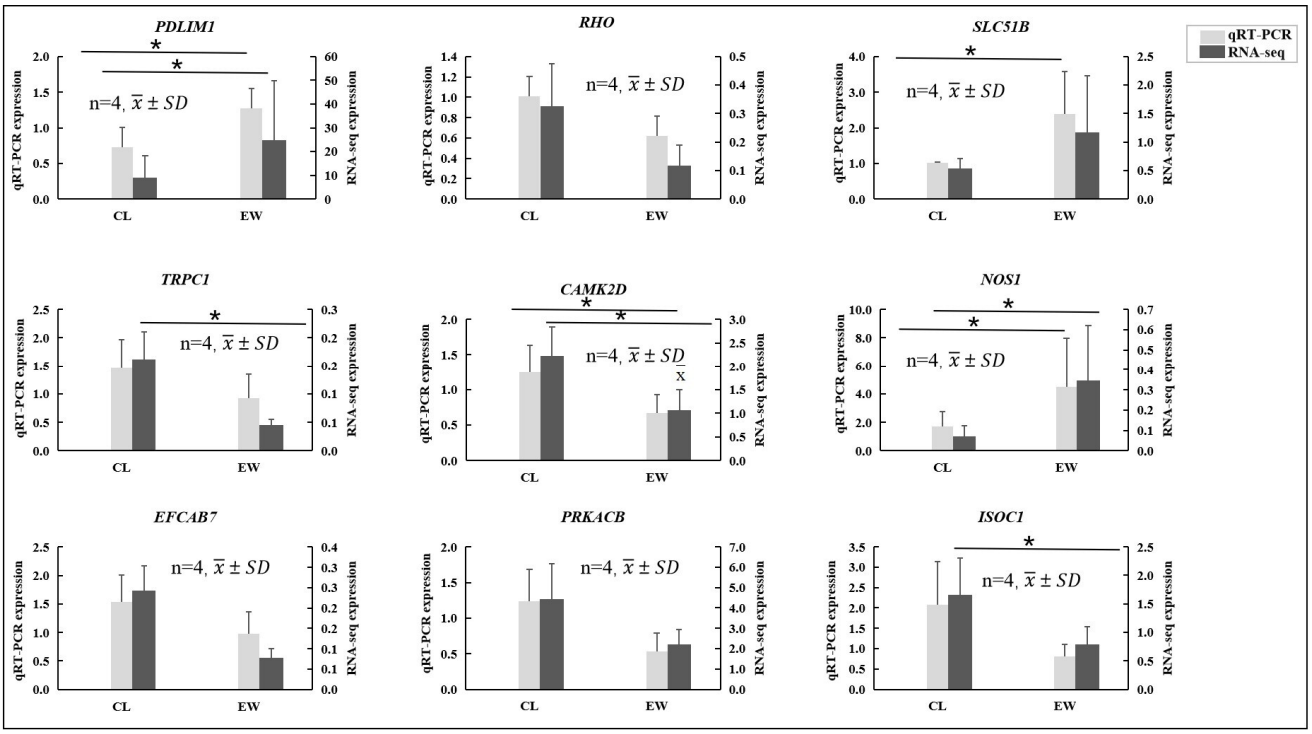

Figure 4. Validation results of qRT-PCR. The left vertical axis represents qRT-PCR relative expression. The right vertical axis represents RNA-seq expression. The left vertical axis represents the relative qRT-PCR expression, and the right vertical axis represents the RNA-seq expression. * denotes significant difference ($p < 0.05$).

4. Discussion

4.1. Analysis of the Visual Function Impact of the YFPs

In this study, we found that the visual function DEGs of the YFPs in ex situ waters and the controlled environment were significantly enriched. Turbidity is an important factor affecting the visual function of aquatic organisms [26]. The visual system of aquatic organisms that live in muddy waters for a long time are degraded to some extent. For example, Indus dolphins in the muddy Ganges and Indus Rivers have small eyes, no lenses, and almost no visual function [27,28]. After the YFPs moved from ex situ waters to the controlled environment, the transparency of the water increased significantly, and their visual regulation showed responsive changes. Enrichment analysis found that the vision-related pathways, such as the inflammatory mediator regulation of TRP channels and phototransduction, were activated in the controlled environment population, and the expression of several vision-related genes, such as *TRPC*1 and *RHO*, was significantly increased ($p \leq 0.05$).

These two genes have been shown to play important roles in the photoconversion of photoreceptor cells and the maintenance of mammalian retinal functions [29,30]. *TRPC1* is an important ion channel protein, which is involved in retinal angiogenesis and lumen formation [31] and plays an important role in photoelectric conversion and other visual aspects [30,32]. Other studies found that retinal pigment epithelial cells (RPE) are mainly driven by the TRPC1 and *TRPC4* channels to drive Ca^{2+} inflow to maintain the normal operation of various Ca^{2+} dependent functions in RPE cells [33]. Lopez (2017) found that *TRPC1* can be expressed in platelets for the regulation of Ca^{2+} entry into retinal cells [34]. *RHO* gene-encoded rhodopsin is a photosensitive pigment in the retina, which can absorb light signals and convert them into chemical signals [35] and is the starting point for the phototransduction pathway [29]. Previous research has found that knocking out the *RHO* gene in macaques leads to retinal pigment degeneration, which, in turn, leads to a significant deterioration in the electroretinogram response and impaired visual ability [29]. Similarly,

RHO is also expressed in animal blood, and the rhodopsin it encodes binds to a protein similar to arrestin in blood cells to thereby regulate phototransduction [36]. In addition, Petersen (2017) developed and validated a digital ELISA method for the quantification of rhodopsin in plasma and found that more diabetic patients with diabetic retinopathy showed blood concentrations of rhodopsin above the limit of detection compared to those of the diabetic patients without diabetic retinopathy [37]. Roshandel (2019) found that mutations of the *RHO* gene in the blood are relatively frequent in patients with retinitis pigmentosa [38]. It was hypothesized that the vision-related genes and pathways were activated when the YFPs were moved from the ex situ waters with high turbidity to the controlled environment with high transparency, which indicates that the visual function of the controlled environment population improved. In addition, we found that several DEGs were significantly enriched in the tight junction, in which many key genes, such as *CX43* (connection 43), *TJP1* (tight junction protein 1), and *AFDN* (afadin, adherens junction formation factor), were significantly up-regulated in the YFPs in the controlled environment. The "cell connection pathway" is mainly responsible for information transmission between animals' multilayer retina and various cells, and the expression and function of the cell connection are affected by external environmental factors [39], especially the regulation of light [40]. The results showed that after the transformation of the YFPs' environment, the above genes and pathways directly related to visual functions were activated, as were the cellular connectivity pathway and other pathways related to visual regulation, which may play a common role in the enhancement of YFPs' visual function.

4.2. Analysis of the Impact of YFPs Digestion Function

We found that the DEGs of the YFPs in ex situ waters and the controlled environment were significantly enriched in the digestive system-related pathways. Similar to other cetaceans [41], the proteins ingested by YFPs are usually initially broken down into polypeptides by gastric acid and pepsin in the stomach, and then further broken down into amino acids by pancreas-secreted proteases, chymotrypsin, elastase, and carboxypeptidase in the small intestine for absorption in the small intestine [42]. In this study, we found that a number of genes related to the digestive system were significantly up-regulated in the controlled environment population. Despite this blood transcriptome analysis result, we found that the expression levels of digestion-related genes in the blood can also reflect the differences in the animals' digestive functions to a certain extent. For example, nitric oxide synthase 1 (*NOS1*) is not only involved in the regulation of gastrointestinal peristalsis and gastric mucus secretion [43], but it also affects the digestive function of animals by regulating the blood supply to the digestive organs [44,45]. In addition to *COL4A1* and *COL4A2*, which also affect the digestive function through the regulation of the blood supply to the digestive organs [46]. And similar studies by Taiwo (2002) found that feeding fenugreek seed extract significantly up-regulated the protein metabolism-related genes in the blood of dairy heifers, resulting in improved energy and amino acid metabolisms, as well as an increased feed intake and digestibility [47]. And our enrichment analysis found that these genes were enriched in the digestive system pathways, such as protein digestion and absorption, gastric acid secretion, and pancreatic secretion, which may indicate that the protein digestive function of the controlled environment population improved.

Under artificial breeding conditions, YFPs receive a stable and regular supply of bait, and the protein and fat contents of the bait is usually high to ensure that they receive a suitable nutritional intake. In ex situ waters, YFPs rely on their own prey to meet their nutritional needs, and the types and quantities of their prey may fluctuate depending on environmental conditions and fish community structure, and prey migration is also uncertain. These differences in feeding may be related to the activation of the protein digestion and absorption pathway in the controlled environment population in this study. Such a finding has been reported before; for example, Mark et al. found that the intake of yellow tail basslet (*Pseudanthias olivaceus*) under random feeding conditions was only 80.9% of that during regular feeding, and the digestive utilization of protein and fat was significantly improved

in the regular feeding group [48]. Yan Hua et al. found that the digestive utilization of fat was higher in North China leopards in controlled environment than it was in wild North China leopards (*Panthera pardus fontanierii*); this is thought to be related to the regular daily intake of North China leopards in the controlled environment [49], suggesting that the regular intake of food could improve their protein digestive utilization. Based on the above results, the YFP controlled environment population showed a certain degree of changes in the feeding conditions, such as regular feeding, so as to maintain high-level protein digestive functions, which was reflected in the activation of the gastric acid secretion and pancreatic fluid secretion pathways in the controlled environment population. Gastric acid is a digestive fluid secreted by the gastric glands distributed in the gastric mucosa, which keeps the pepsin in gastric juice fully energized [50]; pancreatic juice is an exocrine secretion of the pancreas, which is rich in pancreatic proteases [51]. The activation of these two pathways indicated higher protease activity in the controlled environment population of YFPs. This is similar to the results reported by Cheng et al.: the protease, lipase, and amylase activity levels in the intestinal tract of pandas in controlled environment were higher than those of wild pandas [52]. In addition, the mechanical stimulation of food peristalsis promotes an increase in digestive enzyme secretion [53]. The above results suggest that regular feeding is favorable to maintain the digestive tract protease activity at a high level in YFPs, which, in turn, enhances their protein digestion function.

4.3. Analysis of the Immune Function Impact of the YFPs

We found that the DEGs of the YFPs in ex situ waters and the controlled environment were significantly enriched in immune function. Environmental pollutants can trigger an inflammatory response in the body and produce excessive ROS, leading to a state of oxidative stress in the cells, which, in turn, affects the function of the immune system [54,55]. Compared with the controlled environment, the aquatic environment of ex situ waters is more complex and variable. For example, the ex situ waters of the Tian'ezhou National Natural Reserve were contaminated by pesticides and poultry feces from nearby farmland [11]. Mi et al. found that the number of bacterial groups such as Escherichia coli, in the relocated waters of the Yangtze finless porpoises in the ex situ waters of Tongling far exceeded that in the controlled environment [8].

We found that the immune system-related genes were significantly up-regulated in the ex situ population, such as *C1S*, *CCR10*, *PROC*, etc., and were significantly enriched in the chemokine signaling pathway, complement and coagulation cascade, B-cell receptor signaling pathway, etc. Among them, chemokines play an important role in lymphocyte recirculation and inflammatory responses [56]; complement is an important link in immune and inflammatory responses [57]; B cells are important immune cells, and after the body is infected, B cells recognize pathogens and produce specific antibodies through B cell receptors, which then trigger a series of immune responses [58]. It can be seen that the ex situ population may respond to the complex environmental conditions in ex situ waters by activating immune system-related genes and pathways.

5. Conclusions

This study reveals the difference in the expression profiles of the blood transcriptome of Yangtze finless porpoises in ex situ and controlled environments and illustrates the multiple effects and mechanisms of environmental factors on YFPs. The results suggest that the visual and protein digestion functions of the controlled environment population may be improved compared with those of the ex situ population, while the ex situ populations respond to the complex environmental conditions in ex situ waters by enhancing their immune function through the increased expression of immune-related genes. The ex situ protection of Yangtze finless porpoises is an important conservation measure to protect the safety of the species, increase their chances of successful breeding, and expand the population. Since the 1990s, the Ministry of Agriculture and Rural Development in China, together with relevant local governments and research institutes, established five ex situ

populations of Yangtze finless porpoise. Several ex situ protection actions have been carried out since 2015, and the total number of existing ex situ population exceeds 150. The ex situ protection work has achieved remarkable results and become a typical case of international cetacean conservation. For the conservation of Yangtze finless porpoises, artificial breeding is the most effective means to avoid the species extinction. The research on the artificial breeding of Yangtze finless porpoises is significantly dated, and two artificial breeding populations have been established to carry out research on the physiological monitoring and breeding of Yangtze finless porpoises. Tao Tao, born in 2005 at the Wuhan Baiji, is the world's first freshwater cetacean to be successfully bred in a controlled environment. In conclusion, ex situ conservation and artificial breeding are two different and equally important conservation strategies, each with their own emphasis. Therefore, the protection of YFPs requires the selection of appropriate protection methods according to the specific situation, and various factors can be comprehensively considered in order to realize the best outcome.

Supplementary Materials: The following supporting information can be downloaded at: https://www.mdpi.com/article/10.3390/fishes8120593/s1. Figure S1: Amplification curves; Figure S2. Melting curves; Figure S3: KEGG Pathway; Table S1: Morphological information of Yangtze finless porpoises for transcriptomic analysis; Table S2: qPCR reaction; Table S3: qPCR cycling conditions; Table S4: One thousand, two hundred and one differentially expressed genes in EW vs. CL comparison; Table S5: Two hundred and seventy GO entries; Table S6: Differential gene information for heat mapping; Table S7: Forty-nine KEGG pathway entries.

Author Contributions: Conceptualization, D.Y. and K.L.; data curation, Z.C., D.L., J.Z. and C.Y.; formal analysis, Z.C. and H.Z.; funding acquisition, P.X., D.L. and K.L.; investigation, Z.C.; methodology, Z.C. and D.Y.; project administration, G.D. and K.L.; resources, Z.L., Y.Y., P.Z. and S.Z.; software, Z.C., Z.L. and Y.Y.; supervision, G.D. and K.L.; validation, P.X., G.D. and K.L.; visualization, Z.C., D.Y. and Z.H.; writing—original draft, Z.C.; writing—review and editing, D.Y., Y.Y. and K.L. All authors have read and agreed to the published version of the manuscript.

Funding: This project was financed by the Central Public-interest Scientific Institution Basal Research Fund, CAFS (NO. 2023TD11); the Research and Evaluation on the Activity Habits and Habitat Environment of Yangtze Finless Porpoise in Nanjing Yangtze Finless Porpoise Provincial Nature Reserve (2022-JT-005-02); the Scientific Research Monitoring and Dynamic Assessment of Nanjing Yangtze River Dolphin Provincial Nature Reserve (2023-JTYW-07-02); the important environment survey for aquatic organisms in key waters of Anhui Province (ZF2023-18-0236); the Ecological and Environmental Protection Measures for Wuan 6 m Channel Improvement Project—Scientific Examination of Finless Porpoise and Main Habitat Research in Anqing River Section; the National Key R&D Program of China (2022YFF1301604); and the National Key R&D Program of China (2021YFD1200304).

Institutional Review Board Statement: We strictly followed the national regulations and policies for animal protection in China. The medical examinations and related experiments conducted were approved by competent authorities of the Department of Resource Environmental Protection, Yangtze River Basin Fisheries Regulation and Management Office, Ministry of Agriculture. Which reviewed and approved the procedures for animal chasing, handling, and blood collection (2017 [185] and 2018 [183]).

Informed Consent Statement: Not applicable.

Data Availability Statement: mRNA clean transcriptome data were deposited in the NCBI Sequence Read Archive database, with accession number PRJAN1026049.

Conflicts of Interest: Zhanwei Li and Peng Zhang are executives of Zhuhai Chimelong Investment & Development Co. Ltd., Guixin Dong is the executive of Guangdong South China Rare Wild Animal Species Conservation Center. These two companies are subsidiaries of the Chimelong Group and cooperate with the Freshwater Fisheries Research Center to conduct research on the breeding and protection of the Yangtze finless porpoise under the coordination and organization of the management department. And the companies provides us with resources, such as venues and

management. Zhanwei Li, Peng Zhang and Guixin Dong had no role in the the collection, analyses, or interpretation of data, in the writing of the manuscript, or in the decision to publish the results.

References

1. Zhou, X.; Guang, X.; Sun, D.; Xu, S.; Yang, G. Population genomics of finless porpoises reveal an incipient cetacean species adapted to freshwater. *Nat. Commun.* **2018**, *9*, 1276. [CrossRef]
2. Zhang, X.F.; Liu, R.J. The population of finless porpoise in the middle and lower reaches of Yangtze River. *Acta Theriol. Sin.* **1993**, *4*, 005.
3. Wang, D.; Turvey, S.; Zhao, X.; Mei, Z. *Neophocaena asiaeorientalis ssp. asiaeorientalis. The IUCN Red List of Threatened Species*, Version 3.1; IUCN: Gland, Switzerlandand; Cambridge, UK, 2013.
4. Zhao, X.; Barlow, J.; Taylor, B.L.; Pitman, R.L.; Wang, K. Abundance and conservation status of the Yangtze finless porpoise in the Yangtze River, China. *Biol. Conserv.* **2008**, *141*, 12. [CrossRef]
5. Oliveira, M.J.; Aguiar, S.F.H.; Moraes, W.T.; Sanaiotti, M.; Banhos, A.; Moreira, N. Ex situ population of the Harpy Eagle and its potential for integrated conservation. *Zookeys* **2022**, *1083*, 109–128. [CrossRef]
6. Liu, Z.G. *The Changes of Micro-Ecological of Diseased Yangtze Finless and Research on Its Protection under Ex-Situ*; Huazhong Agricultural University: Wuhan, China, 2020.
7. Ye, Q.; Tan, J.; Liu, K. Current status of zooplankton community and assessment of fishery potential in Yangtze finless porpoise ex-situ nature reserve of Xijiang River in Anqing. *Anhui Agric. Sci.* **2021**, *49*, 19.
8. Mi, L.; Yu, D.P.; Jiang, W.H.; Zhou, F. Water quality analyzing of rearing Yangtze finless porpoise in semi-nature reserve. *J. Anhui Univ.* **2003**, *4*, 93–97+110.
9. Hou, Y. Breeding and observation of the Yangtze finless porpoise (*Neophocaena phocaenoides*). *Aquaculture* **1993**, *3*, 13–17.
10. Lin, G.; Hao, Y.J.; Wang, D. Determinaton of serum amino acid concentration in free-ranging and captive Yangtze finless porpoise (*Neophocaena phocaenoides asiaeorientalis*). *Acta Hydrobiol. Sin.* **2008**, *2*, 244–251. [CrossRef]
11. Nabi, G.; Li, Y.; McLaughlin, R.W.; Mei, Z.; Wang, K.; Hao, Y.; Zheng, J.; Wang, D. Immune Responses of the Critically Endangered Yangtze Finless Porpoises (*Neophocaena asiaeorientalis* ssp. *asiaeorientalis*) to Escalating Anthropogenic Stressors in the Wild and Seminatural Environments. *Front. Physiol.* **2019**, *10*, 1594. [CrossRef]
12. Liu, W.; Yin, D.H.; Lin, D.Q.; Yan, Y.; Zhu, X.Y.; Ying, C.P.; Zhang, J.L.; Xu, P.; Liu, K. Blood Transcriptome Analysis Reveals Gene Expression Differences between Yangtze Finless Porpoises from Two Habitats: Natural and Ex Situ Protected Waters. *Fishes* **2022**, *7*, 96. [CrossRef]
13. Sheng, H.B.; Li, C.W.; He, M.; Wu, H.L.; Hang, Y.; Fan, Z.X.; Yue, B.S.; Zhang, X.Y. Transcriptome analysis of the blood of bald male giant pandas (*Ailuropoda melanoleuca*). In Proceedings of the 8th Western China Zoological Symposium, Sichuan, China, 17 November 2023.
14. Liu, G. Immune System and High-Altitude Adaptation Study in Wolf (*Canis lupus*) Based on Blood Transcriptome Analysis. Ph.D. Thesis, Northeast Forestry University, Harbin, China, 2017.
15. Hao, Y.J.; Zhao, Q.Z.; Wu, H.P.; Chen, D.Q.; Gong, C.; Li, L.; Wang, D. Physiological responses to capture and handling of free-ranging male Yangtze finless porpoises (*Neophocaena phocaenoides asiaeorientalis*). *Mar. Freshw. Behav. Physiol.* **2009**, *42*, 315–327. [CrossRef]
16. Kim, D.; Langmead, B.; Salzberg, S.L. HISAT: A fast spliced aligner with low memory requirements. *Nat. Methods* **2015**, *12*, 357–360. [CrossRef]
17. Wang, L.; Feng, Z.; Wang, X.; Wang, X.; Zhang, X. DEGseq: An R package for identifying differentially expressed genes from RNA-seq data. *Bioinformatics* **2010**, *26*, 1. [CrossRef]
18. Stefano, A.F. hypeR: An R package for geneset enrichment workflows. *Bioinformatics* **2020**, *36*, 1307–1308.
19. Du, L.; Liu, Q.; Shen, F.; Fan, Z.; Hou, R.; Yue, B.; Zhang, X. Transcriptome analysis reveals immune-related gene expression changes with age in giant panda (*Ailuropoda melanoleuca*) blood. *Aging* **2019**, *11*, 249–262. [CrossRef]
20. Berkun, L.; Slae, M.; Mor-Shaked, H.; Koplewitz, B.; Eventov-Friedman, S.; Harel, T. Homozygous variants in MAPRE2 and CDON in individual with skin folds, growth delay, retinal coloboma, and pyloric stenosis. *Am. J. Med. Genetics. Part A* **2019**, *179*, 2454–2458. [CrossRef]
21. Anney, P.; Thériault, M.; Proulx, S. Hydrodynamic forces influence the gene transcription of mechanosensitive intercellular junction associated genes in corneal endothelial cells. *Exp. Eye Res.* **2021**, *206*, 108532. [CrossRef]
22. Sin, W.; Haas, K.; Ruthazer, E.S.; Cline, H.T. Dendrite growth increased by visual activity requires NMDA receptor and Rho GTPases. *Nature* **2002**, *419*, 475–480. [CrossRef]
23. Thébault, S. Minireview: Insights into the role of TRP channels in the retinal circulation and function. *Neurosci. Lett.* **2021**, *765*, 136285. [CrossRef]
24. Stavenga, D.G.; Grip, W. Progress in phototransduction. *Biophys. Struct. Mech.* **1983**, *9*, 225–230. [CrossRef]
25. Kahn, B.; Corman, T.; Lovelace, K.; Hong, M.; Krauss, R.; Epstein, D.J. Prenatal ethanol exposure in mice phenocopies Cdon mutation by impeding Shh function in the etiology of optic nerve hypoplasia. *Dis. Models Mech.* **2017**, *10*, 29–37.
26. Davies, C.R.; Nagels, J.; Lydiard, E. Stormflow-dominated loads of faecal pollution from an intensively dairy-farmed catchment. *Water Sci. Technol.* **2008**, *57*, 1519–1523. [CrossRef]

27. Herald, E.S.; Brownell, R.L.; Frye, F.L.; Morris, E.J.; Evans, W.E.; Scott, A.B. Blind River Dolphin: First Side-Swimming Cetacean. *Science* **1969**, *166*, 3911. [CrossRef]
28. Pilleri, G. The blind Indus dolphin, Platanista indi. *Endeavour* **1979**, *3*, 2. [CrossRef]
29. Li, S.Z. *Generation of Nonhuman Primate Retinitis Pigmentosa Model by Knockout of RHO In Vivo*; University of Science and Technology of China: Hefei, China, 2020.
30. Liu, T.T.; Bi, H.S. Advance on transient receptor potential channels in ophthalmology. *Recent Adv. Ophthalmol.* **2009**, *29*, 395–397.
31. Lang, H.B. *Effects of TROC1, 3, and 6 on High Glucose-Induced Human Retinal Vascular Endothelial Cells and Its Mechanism*; Guangxi Medical University: Nanning, China, 2019.
32. Wang, S.Y. *Expression of TRPC Channels in Rat Retina and the Effects of TRPC6 on Retinal Ganglion Cell Apoptosis in Rat Chronic Ocular Hypertension Model*; Fudan University: Shanghai, China, 2014.
33. Wimmers, S.; Strauss, O. Basal Calcium Entry in Retinal Pigment Epithelial Cells. *Investig. Ophthalmol. Vis. Sci.* **2007**, *48*, 13.
34. Lopez, J.J.; Salido, G.M.; Rosado, J.A. Cardiovascular and Hemostatic Disorders: SOCE and Ca^{2+} Handling in Platelet Dysfunction. *Adv. Exp. Med. Biol.* **2017**, *993*, 453–472.
35. Li, J.; Mei, Y. The progress of Rhodopsin in light induced retina degeneration. *Sichuan J. Anat.* **2011**, *19*, 46–48.
36. Scheuring, U.; Franco, M.; Fievet, B.; Guizouarn, H.; Mirshahi, M.; Faure, J.P.; Motais, R. Arrestin from nucleated red blood cells binds to bovine rhodopsin in a light-dependent manner. *FEBS Lett.* **1990**, *276*, 192–196. [CrossRef]
37. Petersen, E.R.B.; Olsen, D.A.; Christensen, H.; Hansen, S.B.; Christensen, C.; Brandslund, I. Rhodopsin in plasma from patients with diabetic retinopathy—Development and validation of digital ELISA by Single Molecule Array (Simoa) technology. *J. Immunol. Methods* **2017**, *446*, 60–69. [CrossRef]
38. Roshandel, D.; Rafati, M.; Khorami, S.; Novin, B.N.; Jalali, S.; Tabatabaie, R.; Rezai, S.; Ahmadieh, H.; Ghaffari, S.R. Rhodopsin gene mutation analysis in Iranian patients with autosomal dominant retinitis pigmentosa. *Int. Ophthalmol.* **2019**, *39*, 2523–2531. [CrossRef]
39. Sakamoto, T.; Sakamoto, H.; Sheu, S.J.; Gabrielian, K.; Ryan, S.J.; Hinton, D.R. Intercellular gap formation induced by thrombin in confluent cultured bovine retinal pigment epithelial cells. *Investig. Ophthalmol. Vis. Sci.* **1994**, *35*, 2.
40. Wang, F.X.; He, S.Z. Advances in the study of retinal intercellular gap junctions. *J. Chin. PLA Postgrad. Med. Sch.* **2006**, *2*, 155–157.
41. Wang, Z.F. *Evolution of Cetacean fat Metabolism-Related Genes and Their Relationship to Aquatic Adaptation*; Nanjing Normal University: Nanjing, China, 2016.
42. Li, G.T. *Genetic Basis of Cetacean Dietary Shifts*; Nanjing Normal University: Nanjing, China, 2018.
43. Martín, M.J.; Jiménez, M.D.; Motilva, V. New issues about nitric oxide and its effects on the gastrointestinal tract. *Curr. Pharm. Des.* **2001**, *7*, 881–908. [CrossRef]
44. Pautz, A.; Li, H.; Kleinert, H. Regulation of NOS expression in vascular diseases. *Front. Biosci.* **2021**, *26*, 85–101.
45. Zhou, L.Q.; Zhu, D.; Tang, Y.D. The history, current status, and direction of cardiovascular metabolic medicine. *Chin. Med. J.* **2022**, *30*, 2389–2393.
46. Yang, W.; Liang, N.F.; Chan, K.; Pu, X.Y.; Poston, R.N.; Ren, M.X.; An, W.W.; Zhang, R.X.; Wu, J.C.; Yan, S.Y.; et al. Coronary-Heart-Disease-Associated Genetic Variant at the COL4A1/COL4A2 Locus Affects COL4A1/COL4A2 Expression, Vascular Cell Survival, Atherosclerotic Plaque Stability and Risk of Myocardial Infarction. *PLoS Genet.* **2016**, *12*, 7. [CrossRef]
47. Taiwo, G.; Sidney, T.; Idowu, M.; Eichie, F.; Karnezos, T.P.; Ogunade, I.M. Dietary fenugreek seed extract improves dry matter intake, apparent total tract nutrient digestibility, and alters whole blood transcriptome of Holstein dairy heifers. *Transl. Anim. Sci.* **2022**, *6*, 4. [CrossRef]
48. Mark, A.; Pirozzi, I. The interaction of feeding regime and dietary specification on growth and nutrient utilisation in Yellowtail Kingfish Seriola lalandi. *Aquaculture* **2021**, *544*, 737094.
49. Hua, Y.; Cao, H.; Wang, J.; He, F.P.; Jiang, G.S. Gut microbiota and fecal metabolites in captive and wild North China leopard (*Panthera pardus japonensis*) by comparsion using 16 s rRNA gene sequencing and LC/MS-based metabolomics. *BMC Vet. Res.* **2020**, *16*, 1. [CrossRef]
50. Richter, P.; Sebald, K.; Fischer, K.; Behrens, M.; Schnieke, A.; Somoza, V. Bitter Peptides YFYPEL, VAPFPEVF, and YQEPVL-GPVRGPFPIIV, Released during Gastric Digestion of Casein, Stimulate Mechanisms of Gastric Acid Secretion via Bitter Taste Receptors TAS2R16 and TAS2R38. *J. Agric. Food Chem.* **2022**, *70*, 11591–11602. [CrossRef] [PubMed]
51. Vertiprakhov, G.V.; Grozina, A.A. Pancreatic Exocrine Function in Chickens. *Russ. Agric. Sci.* **2019**, *45*, 1. [CrossRef]
52. Cheng, M.; Zou, S.Z.; Liao, S.T. Characteristics of Intestinal Micro-ecological Environment of Wild and Captive Giant Pandas and their differences. *J. China West Norm. Univ.* **2020**, *41*, 117–124.
53. Xie, X.J.; Deng, L.; Zhang, B. Advance and studies on ecophysiological effects of starvation on fish. *Acta Hydrobiol. Sin.* **1998**, *22*, 181–188.
54. Wei, S.H.; Zhang, X.N.; Ru, S.G. Advance in visual impairment caused by environmental pollutants in fish. *Asian J. Ecotoxicol.* **2021**, *16*, 104–119.
55. Dong, N.; Guo, H.R.; Wang, Z.C.; Yang, Y.X. Establishment of inflammatory model of lamb peripheral blood mononuclear cells induced by *Escherichia coli* lipopolysaccharide in Vitro. *Acta Ecol. Anim. Domastici* **2022**, *43*, 52–58.
56. Liu, Z.G.; Chen, X.F. Progress of chemokine superfamily. *Chin. Bull. Life Sci.* **1996**, *3*, 1–7.

57. Xu, F. Progress in the study of complement. *Prog. Physiol. Sci.* **1979**, *3*, 207–216.
58. Rahul, N.; Parham, R.; Maximilian, M.; Cihangir, D.; Leandro, C.; Huimin, G.; Sinisa, D.; Hassan, J.; Hilda, Y.B.; Ari, M.; et al. Pre-B cell receptor-mediated activation of BCL6 induces pre-B cell quiescence through transcriptional repression of MYC. *Blood* **2011**, *118*, 15.